expected for a in a given application should be used. The value of a along the trajectory differs from a_1 also to a very small extent due to the deviation of θ from Θ along the trajectory. It is then possible to expand $G(R'+a)$ as follows:

$$G(R'+a)=G(R_t'+a_1)\times\left\{1-\zeta_1\left[\frac{\Delta\cos\Theta}{H}+\frac{(S'-S_t')\cos\Theta}{H}+\frac{1}{H}\frac{da}{d\theta}(\theta-\Theta)\cos\Theta\right]+\tfrac{1}{2}\left(1+\frac{1}{n}\right)\times\zeta_1^2\left[\left(\frac{\Delta\cos\Theta}{H}\right)^2+\frac{2(S'-S_t')\Delta\cos^2\Theta}{H^2}\right]\right\}, \quad (36)$$

where ζ_1 is the following function:

$$\zeta_1=nH[Z+(R+a_1)\cos\Theta]^{-1}. \quad (37)$$

After substitution of Eq. (36) into Eq. (34), and some further manipulation and simplification, one obtains an expression of the following form for the intensities:

$$i_\sigma(R,\Theta)=\tfrac{1}{2}A(nH)^{-n}\cos^{n-1}\Theta\int_0^H[1+\tfrac{1}{2}\sigma\delta(R_t',a_t)]\times\Psi(Z,R,\cos\Theta)[1+\text{other terms}]dZ, \quad (38)$$

where

$$\Psi(Z,R,\cos\Theta)=\zeta_1^n\exp\left[-\left(\frac{H-Z}{L}-\lambda_0\right)\sec\Theta-\alpha_0\right]. \quad (39)$$

Now $\frac{1}{2}\delta$ is quite small compared to unity, and hence if we define a weighted average of δ as

$$\bar{\delta}(R,a_t)=\frac{\int_0^H\Psi(Z,R,\cos\Theta)\delta(R_t',a_t)dZ}{\int_0^H\Psi(Z,R,\cos\Theta)dZ}, \quad (40)$$

we may write to an excellent order of approximation

$$i_\sigma(R,\Theta)=\tfrac{1}{2}A(nH)^{-n}\cos^{n-1}\Theta[1+\tfrac{1}{2}\sigma\bar{\delta}(R,a_t)]\times\int_0^H\Psi(Z,R,\cos\Theta)[1+\text{other terms}]dZ. \quad (41)$$

The integral in Eq. (41) can be evaluated numerically term by term, and the result, after further manipulation,[18] is Eq. (10) of the text.

PHYSICAL REVIEW VOLUME 100, NUMBER 1 OCTOBER 1, 1955

Scattering of Pions by Hydrogen at 165 Mev*

H. L. ANDERSON AND M. GLICKSMAN†
Institute for Nuclear Studies, The University of Chicago, Chicago, Illinois

(Received April 13, 1955)

Measurements of the elastic scattering of both positive and negative pions, and of the charge exchange scattering of negative pions were carried out at each of five angles, at 165 Mev using a liquid hydrogen target. In addition, the total cross sections for positive and negative pions were measured by the transmission method. Integration of the differential measurements gave total cross sections of 199±11 mb for the positive, and 69.8±3.8 mb for the negative pions. The corresponding cross sections obtained by transmission were 188.2±5.4 mb and 67.5±1.5 mb, respectively.

A least squares analysis was carried out on the seventeen data to determine the most probable values of the phase shifts, limiting the analysis to s and p waves. Seven solutions were found, three being of the Fermi type, the others of the Yang type. The Fermi type solutions gave α_{33} near 63°, α_3 near −20°, with the other phase shifts small.

INTRODUCTION

MUCH of the knowledge which we now have about the nature of the interaction between pions and nucleons has come from experiments on the scattering of pions by protons. In interpreting these experiments, the practice has been to carry out a phase shift analysis[1–7] of the data so as to be able to specify the magnitude of the interaction in each of the possible states of the pion-proton system. This program has been hampered considerably by the lack of sufficiently complete and accurate data in general, and of positive pion data above 135 Mev, in particular. Because of this, it was possible to obtain good fits to the experimental data with a number of different phase shift solutions, so that the whole analysis remained somewhat ambiguous.

The present work is part of a program to improve the knowledge of the phase shifts by carrying out more careful measurements with both π^+ and π^- pions. This report covers the experiments carried out at 165 Mev and includes a phase shift analysis of these data.

* Research supported by a joint program of the Office of Naval Research and the U. S. Atomic Energy Commission.

† Present address: RCA Laboratories, Princeton, New Jersey.

[1] Anderson, Fermi, Martin and Nagle, Phys. Rev. **91**, 155 (1953) (Quoted as *A*).

[2] Bodansky, Sachs, and Steinberger, Phys. Rev. **93**, 1367 (1954).

[3] Fermi, Metropolis, and Alei, Phys. Rev. **95**, 1581 (1954).

[4] de Hoffmann, Metropolis, Alei, and Bethe, Phys. Rev. **95**, 1586 (1954).

[5] R. L. Martin, Phys. Rev. **95**, 1606 (1954).

[6] M. Glicksman, Phys. Rev. **94**, 1335 (1954).

[7] J. Orear, Phys. Rev. **96**, 176 (1954).

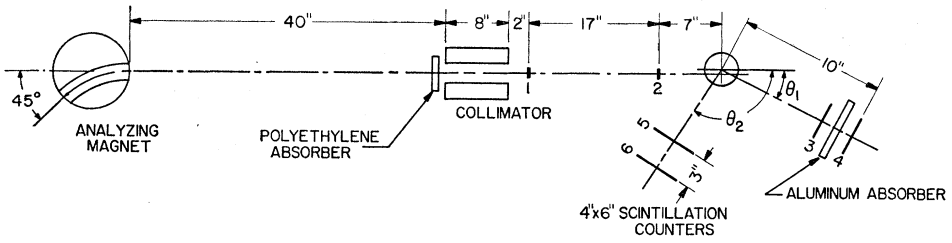

FIG. 1. Arrangement for the elastic scattering of pions by hydrogen. Distances shown are for π^+. For π^- counters 3 and 5 were 10.3 in. and counters 4 and 6 were 20.2 in. from the center of the hydrogen.

EXPERIMENTAL ARRANGEMENT

The arrangement was essentially the same as that used in previous work from this laboratory.[1,6,8,9] Details of the geometry for the elastic scattering are given in Fig. 1. Counters 1 and 2 were plastic scintillators $\frac{1}{8}$ inch thick and 2 inches$\times 2\frac{1}{16}$ inches for the π^+ experiment. For the π^- measurement these were reduced in width from $2\frac{1}{16}$ inches to $1\frac{1}{2}$ inches. Counters No. 3, 4, 5, and 6 were the 4 inch$\times$6 inch liquid scintillators described previously.[1] The use of four such counters made it possible to observe the scattered pions at two angles simultaneously. Proton contamination in the π^+ beam was removed by a 1.48-g/cm^2 polyethylene filter placed at the entrance to an 8-inch collimator in front of counter No. 1.

The charge exchange scattering $\pi^-+P\rightarrow\pi^0+N$ was observed by detecting the gamma rays from the π^0 decay using the anticoincidence technique of Glicksman.[6] The geometry for this experiment is shown in Fig. 2.

In addition to the angular distribution measurements, a transmission measurement was made to obtain the total cross sections in an independent way. The geometry for this is shown in Fig. 3. Counters 3 and 4 were liquid scintillators in Lucite cells having an 8-inch diameter sensitive area.

PION BEAMS

The energy of the pion beams was determined from a range curve in copper using the transmission geometry (Fig. 3) with the hydrogen target removed. For π^+ the mean range was reached by the insertion of 75.3 g/cm^2 of copper in the beam. To obtain the correct value of the range this should be increased by 1.7 g/cm^2 to take into account the multiple scattering of the pions in traversing the copper. This correction was not applied in our previous work.[1,6,8,9] The copper equivalent of the final counters was 4.1 g/cm^2. This includes the addition of 0.3 g/cm^2 to account for the path obliquity in the counters. Thus, the total range was taken to be 81.1 g/cm^2 of Cu. According to Aron's tables,[10] using 6.72 as the ratio of proton to pion mass, we find that pions with this range have an energy of 166.6 Mev. When the hydrogen was in place they lost 1.7 Mev in arriving at the center of the hydrogen so that the energy there was 164.9 Mev. Analysis of the range curve showed, further, an energy spread of 3.7 Mev. With π^- the amount of copper needed to reach the mean range was 74.8 g/cm^2. This was sufficiently close to the result obtained with π^+ that we adopted 165 Mev with an energy spread of ± 6 Mev for both π^+ and π^- experiments.

The muon content of the beam at the center of the hydrogen was estimated, from an analysis of the range curve, to be 4.5 ± 1.0 percent for both π^+ and π^-. The electron content of the beams was negligible.

It was necessary to survey the distribution of the pion beams in space in order to determine the average thickness of hydrogen traversed and to average properly the solid angle subtended by the counters at the hydrogen. This was done by means of a small scintillator $\frac{1}{4}$ inch$\times\frac{1}{4}$ inch in area which could be moved across the beam. From such data we were able to determine that the mean thickness of hydrogen traversed was $(3.699\pm 0.074)\times 10^{23}$ atoms/cm^2 for π^+. In the case of

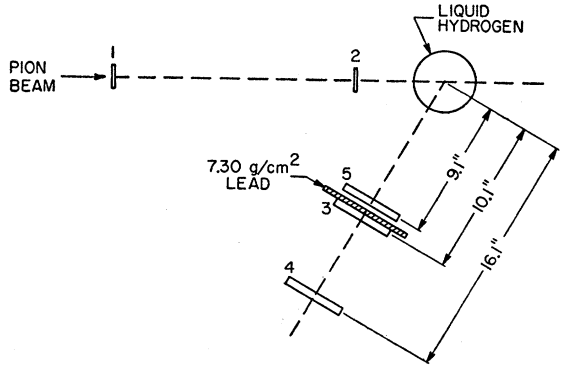

FIG. 2. Arrangement for observing the charge exchange scattering of negative pions in hydrogen.

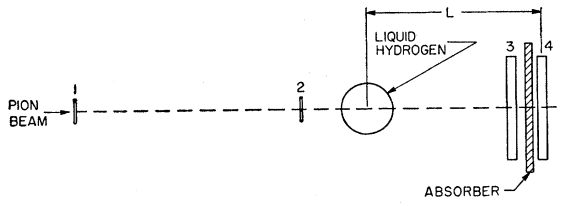

FIG. 3. Transmission method for measuring the total cross section of pions in hydrogen. $L=19.75$ in. for π^-; $L=13.31$ in. for π^+.

[8] Fermi, Glicksman, Martin, and Nagle, Phys. Rev. **92**, 161 (1953).

[9] M. Glicksman, Phys. Rev. **95**, 1045 (1954).

[10] W. A. Aron, University of California Radiation Laboratory Report, UCRL-1325 (unpublished).

π^- a narrower beam was used and the average thickness of hydrogen was $(3.778\pm0.038)\times10^{23}$ atoms/cm^2.

TRANSMISSION EXPERIMENTS

Two transmission measurements were made with π^+. In the first, two 8-inch diameter scintillators were used to detect the transmitted pions with the geometry of Fig. 3. This measures the total cross section for pions scattered at laboratory angles greater than 16.7°. A copper absorber of thickness 8.37 g/cm^2 was inserted between the last two counters so that the scattered protons would not be counted. The ratio of the quadruple coincidence rate with and without hydrogen was found to be

$$R_1=\frac{(Q/D)_{\mathrm{H}}}{(Q/D)_{\mathrm{No\ H}}}=\frac{0.8384\pm0.0019}{0.8929\pm0.0013}=0.9390\pm0.0025.$$

In a second measurement using 4 inch×6 inch counters with 8.78 g/cm^2 of aluminum absorber we obtained

$$R_2=\frac{0.7694\pm0.0011}{0.8196\pm0.0012}=0.9388\pm0.0019.$$

In this case, the measurement included pions scattered at laboratory angles greater than 15.4° on the average.

Under the assumption that the muons in the beam do not interact, and neglecting the effects of multiple Coulomb scattering and of $\pi-\mu$ decay in the liquid hydrogen, the cross section is given by

$$\sigma=-\frac{1}{N}\log_e\left\{R-\frac{r}{T}(1-R)\right\}, \qquad (1)$$

where N is the number of hydrogen atoms/cm^2, r is the ratio of muons to pions in the beam and T is the transmission for pions of the counter and copper absorber assembly used to detect the transmitted particles. For the π^+ measurements $r/T=0.052\pm0.011$.

For the first measurement the cross section turned out to be $(179.4\pm8.3)\times10^{-27}$ cm^2, whereas the second measurement gave $(179.9\pm6.8)\times10^{-27}$ cm^2. The total scattering cross section is obtained by adding the contribution of those pions which are scattered by the hydrogen into the solid angle subtended by the detecting counters. This contribution, excluding the Coulomb scattering, was estimated from the angular distribution measurements. It amounted to $(9.3\pm2.3)\times10^{-27}$ cm^2 for the first, and to $(7.9\pm1.5)\times10^{-27}$ cm^2 for the second transmission measurement. Combining the measurements we obtained

$$\sigma_{\mathrm{total}}(\pi^+)=(188.2\pm5.4)\times10^{-27}\ \mathrm{cm}^2.$$

The transmission measurement with π^- was made with the 8-inch diameter scintillators and a 10.26 g/cm^2 aluminum absorber. In two measurements we obtained

$$R_3=\frac{0.80259\pm0.00040}{0.82180\pm0.00038}=0.97662\pm0.00066,$$

$$R_4=\frac{0.79536\pm0.00028}{0.81476\pm0.00025}=0.97619\pm0.00046.$$

Using $r/T=0.055\pm0.012$ we obtained a cross section of $(66.8\pm1.5)\times10^{-27}$ cm^2 excluding pions scattered by angles less than 11.4°. This contribution, obtained from the angular distribution measurements, amounted to $(0.7\pm0.1)\times10^{-27}$ cm^2 so that the total interaction cross section of π^- with hydrogen was found to be

$$\sigma_{\mathrm{total}}(\pi^-)=(67.5\pm1.5)\times10^{-27}\ \mathrm{cm}^2.$$

These total cross sections are in good agreement with those measured by Ashkin *et al.*[11]

ELASTIC SCATTERING OF POSITIVE PIONS

Measurements of the angular distribution of the scattered pions were made at five different laboratory angles. Using the arrangement of Fig. 1, the scattering was observed at two angles at the same time. Due to the low intensity of the positive pion beam, it was necessary to use large detecting counters rather close to the target in order to obtain acceptable counting rates. This complicated the reduction of the data because the finite size of the detectors and of the target, as well as the variation of the differential cross section with angle had to be taken into account.

The experimental results are collected in Table I, which gives the ratios of quadruple to double coincidences with and without hydrogen in the target, as well as the net effect, taken to be the difference be-

TABLE I. Measurements of elastic scattering of positive pions.

Lab angle θ (degrees)	$(Q/D)_{\mathrm{H}}$ ×10^6	$(Q/D)_{\mathrm{No\ H}}$ ×10^6	$(Q/D)_{\mathrm{net}}$ ×10^6	$\left(\frac{d\sigma}{d\Omega}\right)_{\mathrm{lab}}$ (10^{-27} cm^2/sterad)
30	3234±145	1399±132	1835±196	28.8±3.4
60	1467± 90	557± 70	910±114	12.1±1.6
90	1474± 89	720± 76	754±117	10.0±1.6
120	1490± 91	384± 60	1106±109	15.6±1.8
150	1493± 88	561± 66	932±110	18.5±2.4

TABLE II. Details of the scattering arrangement for π^+.

Laboratory angle θ (degrees)	Distance to last counter d (inches)	Solid angle $\Delta\Omega$ (steradians)	Geometrical factor G	Multiple scattering factor M	Aluminum absorber (g/cm^2)	Detection efficiency ϵ
30	9.94	0.2307	0.964	0.952	8.78	0.876
60	9.89	0.2281	1.016	0.980	2.59	0.937
90	9.87	0.2266	1.039	0.979	0	0.964
120	10.14	0.2180	0.982	0.973	0	0.964
150	12.32	0.1530	0.992	0.975	0	0.964

[11] Ashkin, Blaser, Feiner, Gorman, and Stern, Phys. Rev. **96**, 1104 (1954).

TABLE III. Differential cross sections for 165 Mev π^+ in center of mass system.

Cosine center of mass angle cosχ	Differential cross section $(d\sigma/dw)^+$ (10^{-27} cm^2/sterad)
0.7851	18.7±2.2
0.2793	9.8±1.3
−0.2618	10.7±1.7
−0.6767	21.4±2.5
−0.9209	30.3±3.9

TABLE IV. Observed counting rates in the measurement of the charge exchange scattering.

Lab angle (degrees)	$(Q'D)_H$ ×10^6	$(Q'/D)_{No\ H}$ ×10^6	$(Q'/D)_{net}$ ×10^6
30	254.3±6.8	64.1±4.2	190.2±8.0
60	141.9±6.4	21.4±3.4	120.5±7.3
90	118.2±4.7	20.5±2.6	97.7±5.4
120	136.9±5.2	35.7±3.9	101.2±6.5
150	181.0±6.0	60.5±4.5	120.5±7.5

tween the two. The errors shown are the standard deviations obtained from the total counts observed. The net quadruples to doubles ratio is

$$(Q/D)_{\text{net}}=Nf\epsilon M\sigma(\theta)\Delta\Omega G. \quad (2)$$

In this equation, N is the average number of hydrogen atoms per cm^2 traversed by the beam, f is the fraction of pions in the beam, ϵ is the efficiency of the detector for pions, M is the factor which corrects for the effect of multiple scattering in the target, and $\sigma(\theta)$ is the differential cross section in the laboratory. The solid angle, $\Delta\Omega$, and G, a geometrical factor dependent on $\sigma'(\theta)$ and $\sigma''(\theta)$, are tabulated in Table II. The calculation of $\Delta\Omega$ and G is described in the companion paper.[12] The distance d from the center of the counter to the center of the beam is included in the table, since the beam survey showed a 0.12-inch displacement of its center toward the counters. The counter was 4 inches×6 inches. The effective length of the beam in the target was 3.74 inches, and its cross section was 2 inches×2 inches.

At angles 30° and 60° absorbers were introduced between the last two counters so that the scattered protons would not be recorded. The detection efficiency was calculated taking into account the nuclear interaction of the scattered pions with the materials in their path. For aluminum we used a cross section of 490 millibarns for this and for carbon, 330 millibarns, based on some transmission measurements we had carried out. The efficiencies which were deduced taking these values are listed in Table II.

The multiple scattering correction was made following the method described in the companion paper.[12] The factor M, which is the ratio of single scattering plus in-scattering minus out-scattering to single scattering, was estimated roughly from our knowledge of the energy and angular dependence of the scattering cross section. It will be seen from the values of M listed in Table II that the correction is not very important.

The differential cross sections in the laboratory system were deduced from the observed counting rates using Eq. (2), taking for N the value 3.699×10^{23} hydrogen atoms per cm^2, for f the value 0.955, and for the other quantities, their values as given in Table II. This is the way in which the results listed in the last column of Table I were obtained. The errors quoted were obtained by assigning uncertainties of 2 percent in N, 1 percent in f, 2 percent in ϵ, 2 percent in M, 3 percent in $\Delta\Omega$, and 2 percent in G, and compounding these with the counting errors in the standard way.

Numerical integration of these differential cross sections leads to the value

$$2\pi\int\frac{d\sigma}{d\Omega}d\Omega=(199\pm11)\times10^{-27}\text{ cm}^2.$$

This result is somewhat higher, but not outside the experimental error, than that obtained from the transmission measurement.

The transformation of these results to the center of mass system is given in Table III.

We also fitted these data to an expression of the form

$$d\sigma/dw=a+b\cos\chi+c\cos^2\chi, \quad (3)$$

obtaining, by the method of least squares, the values,

$$a^+=\ 8.85\pm1.18 \text{ millibarns/steradian}$$
$$b^+=-3.66\pm1.76 \text{ millibarns/steradian}$$
$$c^+=\ 21.11\pm3.40 \text{ millibarns/steradian.}$$

CHARGE EXCHANGE SCATTERING OF NEGATIVE PIONS

The measurement of the charge exchange scattering cross sections is complicated by the fact that we cannot observe the neutral pions directly. At best, we can observe the gamma rays into which they decay. This has been done with the anticoincidence arrangement of Fig. 3. The arrangement is not sensitive to charged particles incident on it. Its sensitivity to gamma rays is due principally to the electron pairs which are produced, for the most part, in the lead converter. The data for this experiment are collected in Table IV. In this table Q' is the quadruple coincidence of counters 1, 2, 3, and 4, with counter 5 in anticoincidence, while D is the double coincidence of counters 1 and 2.

In our earlier work we used such data to deduce the differential cross sections for the production of gamma rays by means of a formula analogous to Eq. (2). For the efficiency we used the value calculated for the average gamma-ray energy. This is not quite correct, as Bodansky, Sachs, and Steinberger[2] have shown. The

[12] Anderson, Davidon, Glicksman, and Kruse, following paper [Phys. Rev. **100**, 279 (1955)].

TABLE V. Efficiency for detecting gamma rays.

Gamma ray energy E_γ Mev	Efficiency ϵ for lab angle 30° or 150°	90°
30	0.133	0.130
60	0.363	0.352
90	0.502	0.490
150	0.638	0.628
200	0.676	0.671

gamma rays are emitted over a broad energy spectrum, extending to low energies where the efficiency of the detector is falling rapidly. As a consequence, the efficiency for the average gamma rays is not a good approximation to the average efficiency. In the present work we have, due largely to the insistence of Dr. Jay Orear, attempted to take the energy dependence of the efficiency explicitly into account, in the manner of Bodansky, Sachs, and Steinberger.[2] In this we have been only moderately successful, due to our lack of knowledge of this dependence.

In what follows, we recapitulate the analysis given by Bodansky, Sachs, and Steinberger,[2] in order to make clear the way in which we preferred to deal with the problem.

The differential cross section for neutral pion production in the center of mass system is written as an expansion in Legendre polynomials

$$d\sigma_0/dw_0=\sum_l a_l P(\alpha), \tag{4}$$

where $\cos^{-1}\alpha$ is the center of mass angle of π^0 emission with respect to the incident π^-. In the system in which the π^0 is at rest, the γ rays are emitted isotropically with energy equal to $\frac{1}{2}$ the rest energy of the π^0,

$$E_0=\mu_0 c^2/2. \tag{5}$$

Since two gamma rays are emitted for each π^0 decay, the number emitted into solid angle dw_0 in the rest system of the π^0 will be

$$(1/2\pi)(d\sigma_0/dw_0)dw_0,$$

but in the solid angle dw' of the center of mass system the number of gamma rays will be

$$(1/2\pi)(d\sigma_0/dw_0)(dw_0/dw')dw'.$$

The Lorentz transformation from this system in which the π^0 is at rest to the center of mass system gives

$$dw_0/dw'=1/(\gamma-\eta x)^2, \tag{6}$$

where $\gamma\mu_0 c^2$ is the energy and $\eta\mu_0 c$ is the momentum of the π^0 in the center of mass system, while $\cos^{-1}x$ is the angle of emission of the γ ray with respect to the direction of the π^0 in this system. Thus,

$$\frac{d}{dw}\frac{d}{dw'}\sigma_\gamma(\alpha,x)=\frac{1}{(\gamma-\eta x)^2}\frac{1}{2\pi}\sum_l a_l P_l(\alpha). \tag{7}$$

The number of gamma rays emitted at angle $\cos^{-1}y$ with respect to π^- direction in the center of mass system may be obtained from this by using the addition theorem

$$P_l(\alpha)=\frac{4\pi}{2l+1}\sum_m Y_l^{m*}(x)Y_l^m(y). \tag{8}$$

Then

$$\frac{d}{dx}\frac{d\sigma_\gamma}{dw}=\int\frac{1}{(\gamma-\eta x)^2}\frac{1}{2\pi}\sum_l a_l\frac{4\pi}{2l+1}\times\sum_m Y_l^{m*}(x)Y_l^m(y)d\xi', \tag{9}$$

where $d\xi'$ is the element of polar angle associated with dw'.

$$\frac{d}{dx}\frac{d\sigma_\gamma}{dw}=\sum_l a_l P_l(y)(\gamma-\eta x)^{-2}P_l(x). \tag{10}$$

Transforming to the laboratory system, the factor analogous to (6) is

$$dw/d\Omega=(\gamma_0-\eta_0 z)^{-2}, \tag{11}$$

where η_0/γ_0 is the velocity of the center of mass and $\cos^{-1}z$ is the angle in the laboratory at which the γ rays were observed. We obtain

$$\frac{d}{dx}\frac{d\sigma_\gamma}{d\Omega}=(\gamma_0-\eta_0 z)^{-2}\sum_l a_l P_l(y)(\gamma-\eta x)^{-2}P_l(x). \tag{12}$$

The energy of the gamma rays observed at z depends on the coordinates x and y according to the relation

$$\begin{aligned} E&=E_0(\gamma_0+\eta_0 y)(\gamma-\eta x)^{-1},\\ y&=(\gamma_0 z-\eta_0)(\gamma_0-\eta_0 z)^{-1}, \end{aligned} \tag{13}$$

so that the observed counting rate will be given by

$$\left(\frac{Q}{D}\right)^\gamma=C(\gamma_0-\eta_0 z)^{-2}\sum_l a_l k_l\bar{\epsilon}_l(z)P_l(y), \tag{14}$$

where

$$k_l=\int(\gamma-\eta x)^{-2}P_l(x)dx$$

is the same factor evaluated in A which gives the intensity of the gamma rays belonging to the spherical harmonic of order l. For the present experiment the values are 2, 1.297, and 0.6769, for k_0, k_1, and k_2, respectively.

The explicit dependence of the efficiency on the γ-ray energy occurs in the expression for the average efficiency,

$$\bar{\epsilon}_l(z)=k_l^{-1}\int\epsilon(x,z)(\gamma-\eta x)^{-2}P_l(x)dx. \tag{15}$$

$\epsilon(x,z)$ can be found if $\epsilon(E)$ is known through the use of Eqs. (13).

The factor C is the product of the factors $Nf\Delta\Omega GM$

TABLE VI. Apparent center of mass cross sections for gamma rays due to charge exchange scattering.

Laboratory angle θ (degrees)	$(Q/D)^0\times10^6$	Solid angle $\Delta\Omega$ (sterad)	Geometrical factor G	Multiple scattering factor M	$(\gamma_0-\eta_0 z)^2$	Efficiency $\bar{\epsilon}_0$	$\frac{\bar{\epsilon}_1}{\bar{\epsilon}_0}$	$\frac{\bar{\epsilon}_2}{\bar{\epsilon}_0}$	Apparent center of mass cross section for gammas due to π^0 $\frac{d\sigma^*}{dw}$ (mb/sterad)
30	188.4±8.0	0.0885	0.986	0.989	0.6911	0.558	1.172	1.265	7.49±1.20
60	118.7±7.3	0.0872	1.006	0.992	0.8336	0.536	1.189	1.295	5.88±1.00
90	96.2±5.4	0.0867	1.015	0.990	1.0498	0.505	1.209	1.340	6.36±1.05
120	100.2±6.5	0.0872	0.993	0.989	1.2910	0.490	1.218	1.350	8.55±1.43
150	119.7±7.5	0.0885	0.995	0.989	1.4832	0.472	1.235	1.392	11.97±2.00

which have the same meaning and which are evaluated in the same spirit as the corresponding factors in Eq. (2). Strictly speaking, C depends on l and x and should be incorporated in the integrand of (15). However, in view of the much larger uncertainties involved in estimating $\epsilon(E)$ it would be meaningless to attempt to take this dependence into account. We found it convenient to define an "apparent" cross section for gamma-ray production in the center of mass system

$$\left(\frac{d\sigma_\gamma}{dw}\right)_z^*=\frac{(Q/D)_z{}^\gamma(\gamma_0-\eta_0 z)^2}{Nf\Delta\Omega\epsilon_0(z)MG}, \tag{16}$$

so that we could express the measurements in a form which was convenient for machine calculation of the phase shifts.

$$\left(\frac{d\sigma_\gamma}{dw}\right)_z^*=a_0k_0P_0(y)+a_1k_1\frac{\bar{\epsilon}_1(z)}{\bar{\epsilon}_0(z)}P_1(y)+a_2k_2\frac{\bar{\epsilon}_2(z)}{\bar{\epsilon}_0(z)}P_2(y), \tag{17}$$

limiting the expansion to $l=2$ on the supposition that only s and p waves contribute to the scattering.

In determining the efficiency of our counting arrangement for gamma rays we followed the same general procedure described in A. However, instead of using Wilson's[13] calculations to give the transmission and multiple scattering of the electrons in lead, we carried out some experiments using electrons from our betatron.

The trasmission and multiple scattering of electrons of various energies up to 90 Mev were measured as a function of thickness of lead using a counting geometry similar to that used in the pion scattering work. Further details of these experiments are given in the companion paper.[12] This enabled us to determine the efficiency, especially at low energy, somewhat more reliably than using Wilson's calculations. Nevertheless, these improvements did not remove the major uncertainties in our knowledge of the efficiency and this remains the weakest aspect of our work.

In Table V the efficiency of our counting arrangement for gamma rays is given as a function of gamma-ray energy. The values differ slightly for laboratory angles 30° (or 150°) and 90°, so that the values for 60° (or 120°) could be reckoned by interpolation. From these results the values of $\bar{\epsilon}_0$, $\bar{\epsilon}_1$, and $\bar{\epsilon}_2$ were calculated by numerical integration using Eq. (15). Values of $\bar{\epsilon}_0$ and of the ratios $\bar{\epsilon}_1/\bar{\epsilon}_0$ and $\bar{\epsilon}_2/\bar{\epsilon}_0$ appropriate for the present experiment are tabulated in Table VI.

The counting rates given in the last column of Table IV include a small contribution due to the radiative capture process

$$\pi^-+p\rightarrow n+\gamma.$$

We were able to estimate this contribution from the knowledge of the inverse process,[14] deducing the formula

$$(d\sigma/dw)_{\pi\rightarrow\gamma}=0.072-0.024\cos^2\chi \text{ mb/sterad}$$

by detailed balance. This correction has been included in tabulating the quantity $(Q/D)^0$ in Table VI.

The apparent cross section for the production of gamma rays due to the charge exchange process was calculated using these results by means of Eq. (16). We took $N=3.778\times10^{23}$ atoms/cm^2, $f=0.955$, and other factors as listed in Table VI. Errors were assigned as follows: 1 percent for N, 1 percent for f, 3 percent for $\Delta\Omega$, 15 percent for $\bar{\epsilon}_0$, and 2 percent for MG.

In accordance with Eq. (17) we were able to write the following five relations connecting the experimental results and the coefficients a_0, a_1, and a_2.

Lab angle

$$30^\circ \quad 7.49\pm1.20=2a_0+1.214a_1+0.392a_2, \tag{18a}$$

$$60^\circ \quad 5.88\pm1.00=2a_0+0.488a_1-0.306a_2, \tag{18b}$$

$$90^\circ \quad 6.36\pm1.05=2a_0-0.342a_1-0.389a_2, \tag{18c}$$

$$120^\circ \quad 8.55\pm1.43=2a_0-1.023a_1+0.118a_2, \tag{18d}$$

$$150^\circ \quad 11.97\pm2.00=2a_0-1.461a_1+0.704a_2. \tag{18e}$$

When these equations are solved by the method of least squares the following values are obtained:

$$a_0=\ 3.70\pm0.28,$$
$$a_1=-1.05\pm0.66,$$
$$a_2=\ 3.66\pm1.49.$$

[13] R. R. Wilson, Phys. Rev. 84, 100 (1951).

[14] M. Gell-Mann and K. M. Watson, Ann. Rev. Nuc. Sci. 4, 219 (1954).

TABLE VII. Measurements of the elastic scattering of negative pions.

Lab angle (degrees)	$(Q/D)_H$ $\times 10^6$	$(Q/D)_{No\ H}$ $\times 10^6$	$(Q/D)_{net}$ $\times 10^6$
−29.4	531.7±9.2	451.6±8.3	80.1±12.4
30.0	286.1±8.0	213.6±7.5	72.5±11.0
60.0	77.8±3.0	42.6±2.2	35.2± 3.7
90.0	48.1±2.2	24.4±2.4	23.7± 3.3
120.0	48.2±2.2	24.5±1.7	23.7± 2.8
150.0	81.7±3.6	45.5±2.3	36.2± 4.3

The coefficients a^0, b^0, c^0 appropriate to Eq. (3) are simply related to these and have the values

$$a^0 = 1.87\pm0.76,$$
$$b^0 = -1.05\pm0.66,$$
$$c^0 = 5.49\pm2.24.$$

We can also calculate the integrated value of the cross section due to charge exchange

$$\sigma^0 = \int \left(\frac{\partial\sigma^0}{dw}\right) dw = 4\pi a_0 = (46.5\pm3.5)\times10^{-27}\ \text{cm}^2.$$

The error given here is smaller than it would be if we had not neglected the correlation on the errors assigned to the efficiencies among the relations (8).

ELASTIC SCATTERING OF NEGATIVE PIONS

This experiment was carried out in a manner similar to that for the positive pions. Because of the higher flux which was available it was possible to use a better-defined geometry. This simplified the reduction of the data. The experimental data are given in Table VII. The errors given are the standard deviations due to statistics alone.

A small percentage of the counting rate recorded in the last column of Table VII is due to the gamma-ray production process. This was obtained by estimating the efficiency of this arrangement for detecting gamma rays, and using the data of the gamma-ray measurements. This contribution was subtracted in obtaining the value $(Q/D)^-$ due to the elastic scattering of negative pions alone, given in the second column of Table VIII. Proceeding as for the positive pions we calculated the differential cross sections in the laboratory given in the last column of Table VIII. The error given includes an error of 1 percent in the value of N, an error of 1 percent in the value of f, and errors of 2 percent of ϵ_- and of 2 percent in $\Delta\Omega$.

The total cross section for the elastic scattering of negative pions was calculated by a numerical integration of these results to have the value

$$\sigma(\pi^- \rightarrow \pi^-) = (22.5\pm1.5)\times10^{-27}\ \text{cm}^2.$$

Adding to this the value $(46.5\pm3.5)\times10^{-27}$ cm^2 due to charge exchange and the value $(0.80\pm0.20)\times10^{-27}$ cm^2 due to radiative capture, the total cross section for negative pions obtained in this way is found to have the value

$$\sigma_{\text{total}}(\pi^-) = (69.8\pm3.8)\times10^{-27}\ \text{cm}^2,$$

in reasonable agreement with the result of the transmission measurement.

The differential cross sections for the elastic scattering for the center of mass system are given in Table IX.

PHASE SHIFT ANALYSIS

As in the earlier work,[1] a phase shift analysis of the data was carried out using an electronic computer. We are grateful to Donald Flanders and to Jean Hall of the Argonne National Laboratory for the opportunity to use the AVIDAC for this purpose. As before, the cross sections were expressed in terms of the phase shifts, limiting the analysis to include only s and p waves in states of isotopic spin $\frac{1}{2}$ and $\frac{3}{2}$. Starting with an initial set of six phase shifts, the machine computes the sum

$$M(\alpha_1,\alpha_3,\alpha_{11},\alpha_{13},\alpha_{31},\alpha_{33}) = \sum_{i=1}^{17} \frac{\Delta_i^2}{\epsilon_i^2} \qquad (19)$$

where $\alpha_1, \cdots, \alpha_{33}$ are the six phase shifts with the notation of A, ϵ_i is the experimental error, and Δ_i is the deviation of the calculated from the observed cross section. The machine then proceeds to vary each phase angle in turn, seeking the set which gives the minimum value of M. It first varies α_1 by either plus or minus 1 degree, computes the corresponding value of M, and selects the altered or original value of the phase angle according to which gave the smaller M. It then proceeds to vary the next angle, and the next in order, until no further decrease in M is obtained. The variation is then reduced to $\frac{1}{2}$ degree and the same procedure is re-

TABLE VIII. Scattering of negative pions in the laboratory system.

Lab angle θ (degree)	$(Q/D)^-\times10^6$	Solid angle $\Delta\Omega$ (steradians)	Geometrical factor G	Multiple scattering factor M	Aluminum absorber (g/cm^2)	Detection efficiency ϵ_-	Differential cross section in laboratory system $d\sigma^-/dw$ (10^{-27} cm^2/sterad)
30	70.2±8.3	0.0570	0.991	0.979	8.78	0.835	4.21±0.53
60	31.1±3.7	0.0562	1.004	0.984	2.59	0.907	1.71±0.21
90	20.2±3.3	0.0559	1.009	0.986	0	0.939	1.07±0.13
120	20.0±2.8	0.0562	0.996	0.986	0	0.939	1.08±0.16
150	31.7±4.3	0.0570	0.997	0.987	0	0.939	1.67±0.24

TABLE IX. Differential cross sections for elastic scattering of negative pions in the center of mass system.

Cosine of center mass angle cosχ	Differential cross section $(d\sigma/dw)^-$ (10^{-27} cm²/sterad)
0.7851	2.74±0.34
0.2793	1.38±0.17
−0.2618	1.14±0.19
−0.6767	1.48±0.22
−0.9209	2.74±0.39

peated. The variation is reduced by a factor of two at each stage until it is 2^{-7} degrees. When the machine is unable to reduce M further using this variation it prints out the final set of α's and the corresponding cross sections and stops.

In the present work we required the solution to fit 17 different measurements instead of 9 as previously. These were the differential cross sections for the positive (Table III), negative (Table IX), and charge exchange [Eq. (18)] scattering processes, measured at each of five angles, and the total cross sections of positive and negative pions, obtained from transmission measurements.[15] Thus, the experimental knowledge was more completely exploited here than was possible previously.[3–6]

For the initial values of the phase shifts, we chose sets obtained from the construction of Ashkin diagrams.[16] Such construction utilizes only a part of the experimental data and leads to a multiplicity of possible solutions. The multiplicity can be as large as 16, not counting those solutions which differ only in that the signs of all the phase shifts are reversed. In our construction of these diagrams, we varied the input data as liberally as possible within the limits allowed by the experimental error so as to obtain as many starting sets as was reasonable.

In the Ashkin construction the phase shifts are obtained from the intersection of two circles. Thus, one starts out by finding two possible values for α_3, in the present case, −18.5 degrees and −27 degrees. Each of these leads to two possible sets of values for the pair, α_{33} and α_{31}. That for which α_{33} is large and α_{31} is small is known as the Fermi solution. The other, known as the Yang form, may be obtained from the first by means of the transformation

$$\begin{aligned}\alpha_{33}'&=\eta_3-\alpha_{33},\\ \alpha_{31}'&=\eta_3-\alpha_{31},\end{aligned}\tag{20}$$

where

$$\eta_3=\text{angle of } (2e^{2i\alpha_{33}}+e^{2i\alpha_{31}}).$$

This solution is characterized by an α_{31} which is larger than α_{33}. Each of the four possible solutions for this isotopic spin $\frac{3}{2}$ state leads to two solutions for α_1, and these in turn to possibilities which correspond to the Fermi and Yang sets for the isotopic spin $\frac{1}{2}$ state. It frequently happens that some of the possibilities are not allowed by the data. In the present case we found some 12 possibilities which appeared to be acceptable. These are displayed in Table X. With these as the starting point, the machine found the solutions shown in the same table.

It will be seen that 7 solutions remain even when all the experimental data is included and a least squares fit is demanded. For a given solution, the value of M may serve as a measure of the goodness of the fit. In the usual theory of least squares, where the measurements are truly independent, the errors truly statistical,

TABLE X. Phase shifts at 165 Mev.

α_3	−18.5					−27						
α_{33}	+61.0			+31		+53			+27			
α_{31}	+ 3.5			+89		+ 6			+81			
α_1	+9		− 3	+9		− 3	+8		− 4	+8		− 4
α_{13}	+2	−6	−12	+2	−6	−12	−5	+3	−12	−5	+3	−12
α_{11}	−8	+6	−12	−8	+6	−12	+7	−9	−12	+7	−9	−12
Track	#1	#2	#3	#4	#5	#6	#7	#8	#9	#10	#11	#12
α_3	−20.0	−20.7		−19.9	Same	−19.6	Same	−26.0	Same	−35.5	−28.2	Same
α_{33}	+63.0	+62.1		+33.7	as	+32.7	as	+60.1	as	+27.7	+30.4	as
α_{31}	+ 3.7	+ 1.3		+93.7	#10	+94.2	#2	+ 6.5	#2	+73.0	+82.2	#6
α_1	+ 8.0	− 2.1		+ 9.4		− 1.3		+ 6.8		+ 4.8	+ 8.0	
α_{13}	+ 1.0	− 5.6		+ 0.6		− 7.7		+ 1.7		− 7.8	+ 2.0	
α_{11}	−10.6	−13.1		− 5.6		−10.6		−11.3		+10.6	− 8.0	
M	5.27	5.30		6.08		5.21		5.44		6.25	6.21	

[15] For a variety of reasons the numbers actually fed into the computer differed in minor ways from the final values listed in the tables. The effect on the final results should not be significant.

[16] J. Ashkin and S. H. Vosko, Phys. Rev. **91**, 1248 (1953).

TABLE XI. Calculated cross sections compared with observed values[a] for 165 Mev. Here $\lambda\!\!\!^{-2}=8.874\times10^{-27}$ cm^2.

Quantity	Lab angle	Expt value	Error	Calculated values Solution #1	#2	#6	#8	#10	#11
$4\lambda\!\!\!^{-2}d\sigma^+/dw$	30	8.43	0.99	9.20	9.00	9.02	9.26	9.17	9.38
	60	4.40	0.59	4.02	4.12	4.12	3.98	4.02	4.00
	90	4.79	0.77	4.31	4.38	4.38	4.26	4.20	4.25
	120	9.63	1.12	8.60	8.41	8.42	8.62	8.31	8.64
	150	13.66	1.76	12.79	12.34	12.37	12.87	12.34	12.94
$36\lambda\!\!\!^{-2}d\sigma^-/dw$	30	11.10	1.37	10.91	10.65	10.71	10.96	11.15	11.42
	60	5.59	0.69	5.54	5.41	5.44	5.57	5.27	5.65
	90	4.61	0.77	4.45	4.40	4.41	4.45	4.14	4.33
	120	6.01	0.89	6.82	6.83	6.83	6.81	6.86	6.72
	150	11.11	1.47	9.55	9.58	9.57	9.51	9.93	9.52
$18\lambda\!\!\!^{-2}d\sigma^*/dw$	30	15.86	2.53	14.52	16.43	16.32	14.66	15.07	14.48
	60	12.09	2.01	11.23	11.78	11.55	11.23	12.10	10.97
	90	13.15	2.15	12.73	12.33	12.21	12.65	13.19	12.31
	120	17.48	2.92	18.19	17.52	17.69	18.06	17.69	17.73
	150	24.41	4.05	23.60	22.99	23.43	23.50	22.20	23.15
$4\lambda\!\!\!^{-2}\sigma_T^+$	···	84.83	2.43	85.89	84.92	85.00	85.86	84.30	86.38
$36\lambda\!\!\!^{-2}\sigma_T^-$	···	273.83	6.41	274.02	276.48	276.24	273.94	276.49	271.46

[a] Values given here were used in the machine calculation and differ in minor ways from the values given in the tables above.

and where the derived quantities have a linear dependence on the measured quantities in the vicinity of the solution, the expectation value of M is 11 for fitting 17 independent data with 6 parameters. In the present case these conditions were not well satisfied. An effort was made not to overestimate the errors and thereby exaggerate the goodness of fit. However, the errors do include contributions due to uncertainties in the measurements, not purely statistical in nature. Moreover, the errors quoted for the cross sections are not all independent. The error which occurs in N, the number of hydrogen atoms per cm^2, is common to all the measurements. Errors which appear in the efficiency for detecting gamma rays are common to all the charge exchange cross sections. For these reasons the expectation value should be considerably less than 11. It was not surprising that the solutions found had values of M near 6.

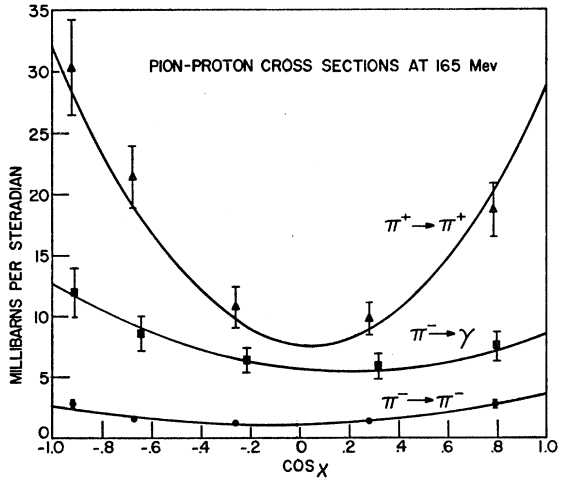

FIG. 4. Scattering of pions by protons at 165 Mev. The curves correspond to solution 1.

It is very difficult to distinguish from these experiments alone, which of the solutions found is the correct one. The values of M found were between 5.21 and 6.25, a variation small compared to the expected rms deviation $\langle(M-\bar{M})^2\rangle_{Av}^{\frac{1}{2}}=(2\bar{M})^{\frac{1}{2}}=3.5$. This is also made clear in Table XI where the values of the cross sections found by the machine for the various solutions are compared with the input values. Study of this table shows that the machine-found values tend to cluster together, indicating that a considerable improvement in the precision of the measurements would be required to make a clear decision in favor of any one of the possible solutions. A comparison of the experimental data with that of solution 1 is given in Fig. 4.

The reason for the multiplicity of solutions which occurs at 165 Mev can be understood, in part, by examining the Ashkin diagram shown in Fig. 5. In Ashkin's procedure the solutions for α_3 are obtained from the intersection of two circles. In the present case, these circles are almost tangent to one another so that the two solutions marked a and b come close together. In fact, all values of α_3 which lie within the shaded region give almost equally good fits to the experimental data. The corresponding values of α_{31} and α_{33} are also shown shaded. Solutions 1, 2, and 8 all fall within the shaded region. The corresponding Yang forms of these are those which fall between the dashed lines of the diagram and include solutions 4, 6, and 11.

SENSITIVITY OF THE PHASE SHIFTS

In order to obtain a better idea as to how well the phase shifts are determined by the experiments, the machine was started with the phase shifts of solution 1 and the phase shifts were then varied either single or in pairs until the value $M=8$ was reached. This made it possible to draw the contours shown in Fig. 6. In first order, these contours should form a 6-dimensional hyper-

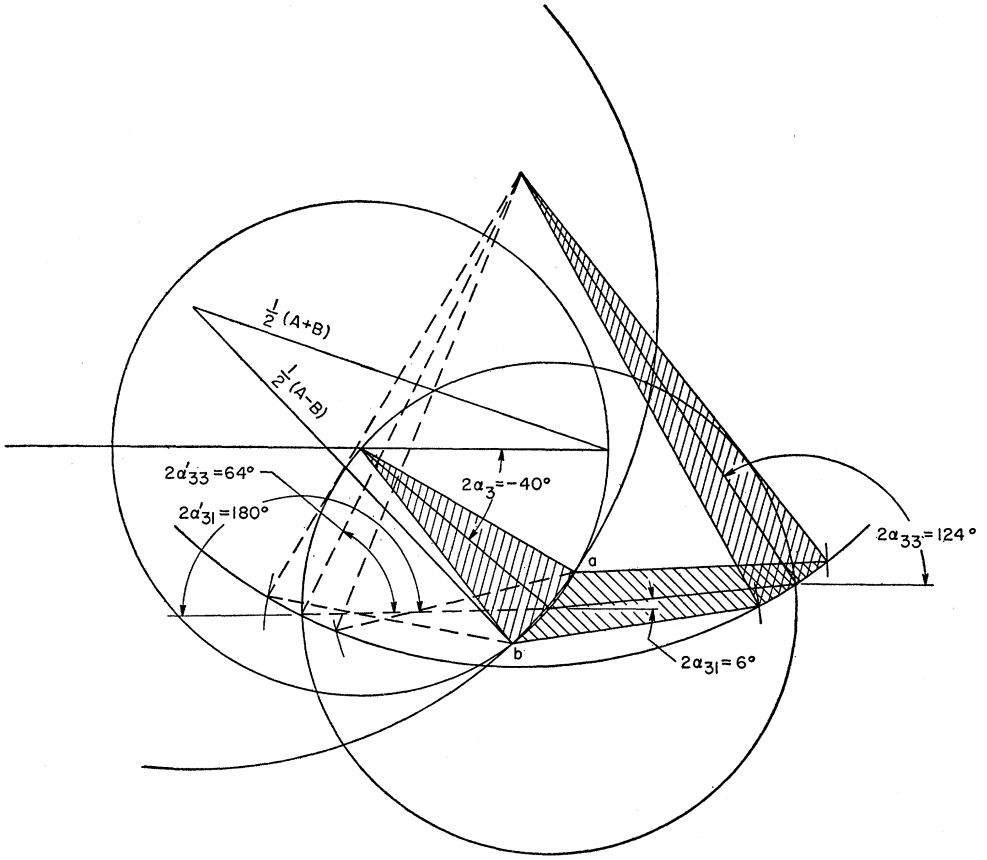

FIG. 5. Ashkin diagram showing spread of possible solutions for α_3. Fermi-type solutions for α_{33} and α_{31} are included in shaded area. Yang-type solutions for α_{33} and α_{31} are included within the dashed lines.

ellipsoid and any set of phase shifts lying within this figure should be acceptable according to the experiments. Figure 6 attempts to show some of the projections of this hyperellipsoid. It shows, in orthographic projection, the ellipsoid corresponding to the isotopic spin $\frac{3}{2}$ state, and separately, that for the isotopic spin $\frac{1}{2}$ state. The elongated form of the ellipses for α_3 and α_{33}, and for α_{31} and α_{33} is due to degeneracy of the solutions for α_3 already referred to.

DISCUSSION

For purposes of discussion, it seems desirable to concentrate the attention on the solutions of the Fermi type, and set aside the solutions of the Yang type. This step receives some justification based on simplicity. The Yang-type solutions have α_{-3} and α_{31} both large, instead of just α_{33} large for the Fermi type. When the Yang-type solutions are followed to higher energy, as has been done by de Hoffmann, Metropolis, Alei and Bethe,[4] and by Martin,[5] they lead to three resonances instead of one for the Fermi-type solution.

Our solution 1 is quite close to the one which de Hoffmann, Metropolis, Alei, and Bethe[4] believe to be the correct one. They analyzed the available negative pion data between 120 and 217 Mev and selected those solutions which varied continuously with energy, and gave positive pion total cross sections in agreement with the experimental values. In their preferred solution, α_{33} goes through 90° at about 195 Mev while the other p phase shifts are small. The same solution was also found by Glicksman[6] by setting $\alpha_{11}=\alpha_{13}=\alpha_{31}=0$.

The choice of interaction corresponding to α_{33} dominant and resonant is the one first proposed by Brueckner[17] to account for the early pion scattering results. The same choice has provided the basis for a successful interpretation of a number of the features of the process of pion production by nucleons as well as by gamma rays. Thus, Brueckner and Watson[18] have pointed out that the angular distribution observed[19] for the reaction $p+p\rightarrow\pi^+ +d$ is not very different from the form $0.3+\cos^2\chi$ which it would have with the $p_{\frac{3}{2}}$ state of the pion-nucleon system dominant. Subsequently, a more detailed study by Rosenfeld[20] and a general review by Gell-Mann and Watson[14] have reaffirmed this point of view. A similar argument operates in the photoproduction process, where again the emission of the pion in the $p_{\frac{3}{2}}$ state would give an isotropic distribution whereas

[17] K. A. Brueckner, Phys. Rev. **86**, 106 (1952).
[18] K. A. Brueckner and K. M. Watson, Phys. Rev. **86**, 923 (1952).
[19] Cartwright, Richman, Whitehead and Wilcox, Phys. Rev. **91**, 677 (1953).
[20] A. H. Rosenfeld, Phys. Rev. **96**, 139 (1954).

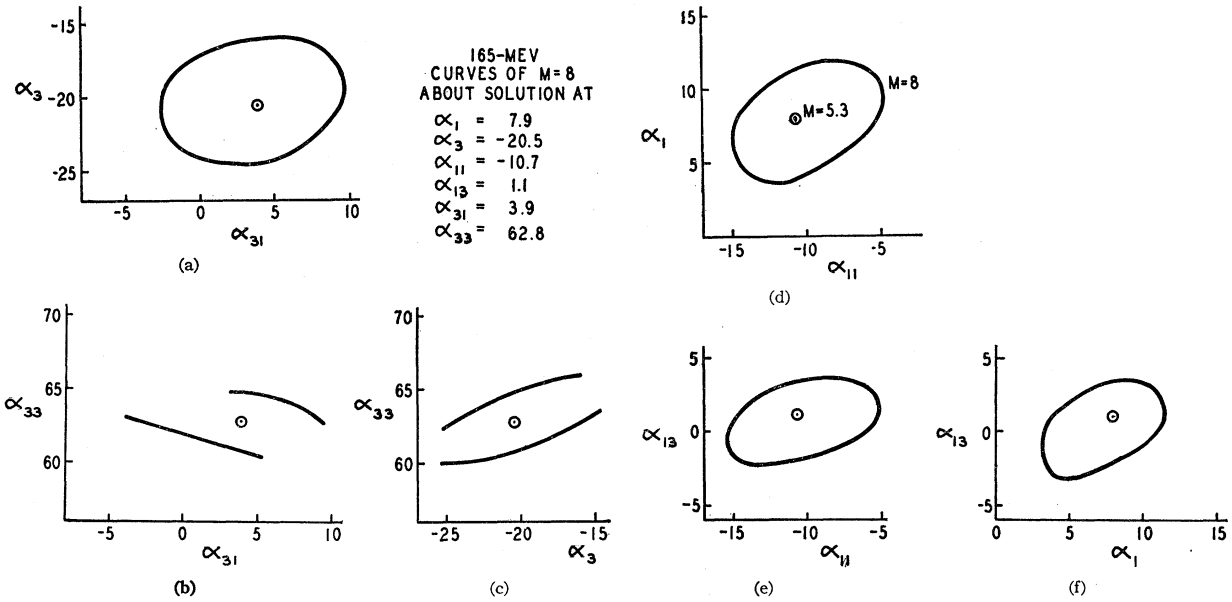

FIG. 6. Orthographic projection of error ellipses of the phase shifts for isotopic spin states $\frac{3}{2}$ and $\frac{1}{2}$.

the actual angular distributions[21] show the marked angular dependence expected from emission in the $p_{\frac{3}{2}}$ state. A noteworthy calculation by Chew[22] based on a static, cut-off, pseudo-vector meson theory, with moderately weak coupling, reproduces quite well the phase shifts given by de Hoffmann *et al.*,[4] and by Glicksman,[6] and at the same time, much of the available photo-pion production data. These qualitative arguments make plausible the choice of solution 1, but they do not finally rule out the other possibilities.

The behavior of α_{33} and of α_3 found by de Hoffmann, Metropolis, Alei, and Bethe[4] is confirmed at 165 Mev by our value for these phase angles. The same can be said of the Fermi-type solutions arrived at by Martin[5] who set $\alpha_{11}=\alpha_{13}=0$, and also the solution of Glicksman[6] who set $\alpha_{11}=\alpha_{13}=\alpha_{31}=0$. Thus the general behavior of α_{33} seems to be rather well determined, at least in the vicinity of 165 Mev and below. This is because the $\frac{3}{2},\frac{3}{2}$ interaction is so dominant.

The behavior of the other phase shifts has been less well established by the analyses carried out thus far. They all have the defect of having neglected the possible effect of d waves. We hope to improve this situation in our future work.

ACKNOWLEDGMENTS

We wish to thank Mr. Tadao Fujii and Mr. Joseph Fainberg for helping to carry out the measurements and Dr. William C. Davidon and Dr. Ulrich Kruse for helping to analyze the data.

[21] A. Silverman and M. Stearns, Phys. Rev. **88**, 1228 (1952); G. Cocconi and A. Silverman, Phys. Rev. **88**, 1230 (1952); Goldschmidt-Clermont, Osborne, and Scott, Phys. Rev. **89**, 329 (1953); Walker, Oakley, and Tollestrup, Phys. Rev. **89**, 1301 (1953).

[22] G. F. Chew, Phys. Rev. **95**, 1669 (1954).